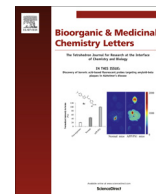




Contents lists available at ScienceDirect

# Bioorganic & Medicinal Chemistry Letters

journal homepage: [www.elsevier.com/locate/bmcl](http://www.elsevier.com/locate/bmcl)

## Synthesis, biological evaluation and molecular docking study of some novel indole and pyridine based 1,3,4-oxadiazole derivatives as potential antitubercular agents



N. C. Desai<sup>a,\*</sup>, Hardik Somani<sup>a</sup>, Amit Trivedi<sup>a</sup>, Kandarp Bhatt<sup>a</sup>, Laxman Nawale<sup>b</sup>, Vijay M. Khedkar<sup>b</sup>, Prakash C. Jha<sup>c</sup>, Dhiman Sarkar<sup>b</sup>

<sup>a</sup> Division of Medicinal Chemistry, Department of Chemistry (DST-FIST Sponsored), Mahatma Gandhi Campus, Maharaja Krishnakumarsinhji Bhavnagar University, Bhavnagar 364 002, Gujarat, India

<sup>b</sup> Combi Chem Bio Resource Centre, National Chemical Laboratory, Pune 411 008, India

<sup>c</sup> School of Chemical Sciences, Central University of Gujarat, Sector-30, Gandhinagar 382 030, Gujarat, India

### ARTICLE INFO

#### Article history:

Received 24 September 2015

Revised 10 February 2016

Accepted 16 February 2016

Available online 16 February 2016

#### Keywords:

Indole  
1,3,4-Oxadiazole  
Pyridine  
Antitubercular activity  
Molecular docking  
Cytotoxicity

### ABSTRACT

A series of indole and pyridine based 1,3,4-oxadiazole derivatives **5a–t** were synthesized and evaluated for their in vitro antitubercular activity against *Mycobacterium tuberculosis* H<sub>37</sub>Ra (MTB) and *Mycobacterium bovis* BCG both in active and dormant state. Compounds **5b**, **5e**, **5g** and **5q** exhibited very good antitubercular activity. All the newly synthesized compounds **5a–t** were further evaluated for anti-proliferative activity against HeLa, A549 and PANC-1 cell lines using modified MTT assay and found to be noncytotoxic. On the basis of cytotoxicity and MIC values against *Mycobacterium bovis* BCG, selectivity index (SI) of most active compounds **5b**, **5e**, **5g** and **5q** was calculated (SI = GI<sub>50</sub>/MIC) in active and dormant state. Compounds **5b**, **5e** and **5g** demonstrated SI values  $\geq 10$  against all three cell lines and were found to be safe for advance screening. Compounds **5a–t** were further screened for their antibacterial activity against four bacteria strains to assess their selectivity towards MTB. In addition, the molecular docking studies revealed the binding modes of these compounds in active site of enoyl reductase (InhA), which in turn helped to establish a structural basis of inhibition of mycobacteria. The potency, low cytotoxicity and selectivity of these compounds make them valid lead compounds for further optimization.

© 2016 Elsevier Ltd. All rights reserved.

Tuberculosis (TB) remains a major global health problem being the second leading cause of death from infectious diseases worldwide, after the human immunodeficiency virus (HIV). Conventional treatments fail either because of poor patient compliance to the drug regimen or due to the emergence of multidrug-resistant tuberculosis (MDR-TB). *Mycobacterium tuberculosis* (MTB) infection is difficult to treat, requiring 6–9 months of chemotherapy with a cocktail of four antibiotics isoniazid, rifampin, pyrazinamide and ethambutol. In addition to toxic side effects, the lengthy treatment regime results in poor patient compliance and thus drug resistant strains are beginning to emerge.<sup>1</sup> In recent years, the emergence of MDR and XDR (extensively drug-resistant) tuberculosis strains has amplified the incidences of TB. In addition, TB is a co-infection of HIV-AIDS (Acquired Immune Deficiency Syndrome) and accounts for 26% of AIDS related death worldwide.<sup>2–6</sup> In 2013, an estimated 9 million people were affected by *M. tuberculosis* and 1.5 million

died from the disease, including 360,000 deaths among HIV-positive patients.<sup>7</sup> To address these problems, it has become inevitable to design, synthesize and develop effective anti-mycobacterial agents are compulsory.

The indole moiety is probably the most widely spread nitrogen heterocycle in nature. It is an essential part of the amino acid tryptophan and the neurotransmitter serotonin, and the indole scaffold is also found in numerous naturally occurring plant based alkaloids. The biological importance of indole heterocycles and their pharmacological and medical potential have made them extremely attractive and rewarding research targets and these qualities have motivated countless researchers to study their synthesis and pharmacological properties.<sup>8</sup> The biological activities of indoles cover a wide spectrum, including anticancer,<sup>9,10</sup> antimicrobial,<sup>10</sup> anti-inflammatory,<sup>11</sup> antimalarial,<sup>12</sup> cytotoxic<sup>12</sup> and antitubercular<sup>13</sup> activities.

The pyridine motif is among the most common N-hetero aromatics incorporated into the structure of various therapeutic agents. Many naturally occurring and synthetic compounds

\* Corresponding author. Tel./fax: +91 278 2439852.

E-mail address: [dnisheeth@rediffmail.com](mailto:dnisheeth@rediffmail.com) (N.C. Desai).

bearing pyridine scaffold possess interesting biological properties. Compounds containing pyridine ring display a broad spectrum of biological activities, including anticancer,<sup>14</sup> antimicrobial,<sup>15</sup> anticonvulsant,<sup>16</sup> antibacterial,<sup>17</sup> anti-inflammatory,<sup>18</sup> antitumor<sup>19</sup> and antiviral<sup>20</sup> activities. On the other hand, compounds containing 1,3,4-oxadiazole ring display a broad spectrum of biological activities, including anticancer,<sup>21</sup> antimicrobial and cytotoxic,<sup>22</sup> anticonvulsant,<sup>23</sup> antiepileptic,<sup>24</sup> antitubercular<sup>25</sup> and anti-allergic<sup>26</sup> activities. 1,3,4-Oxadiazole is a good bioisostere of amide and ester functional groups and is reported to contribute substantially to pharmacological activity by participating in hydrogen bonding interactions with various receptors.<sup>27</sup> On the basis of the principle of combination of active structural moieties, it is reported that substitution by oxadiazoles at the 3-position of the indole nucleus enhances the biological activities.<sup>28,29</sup>

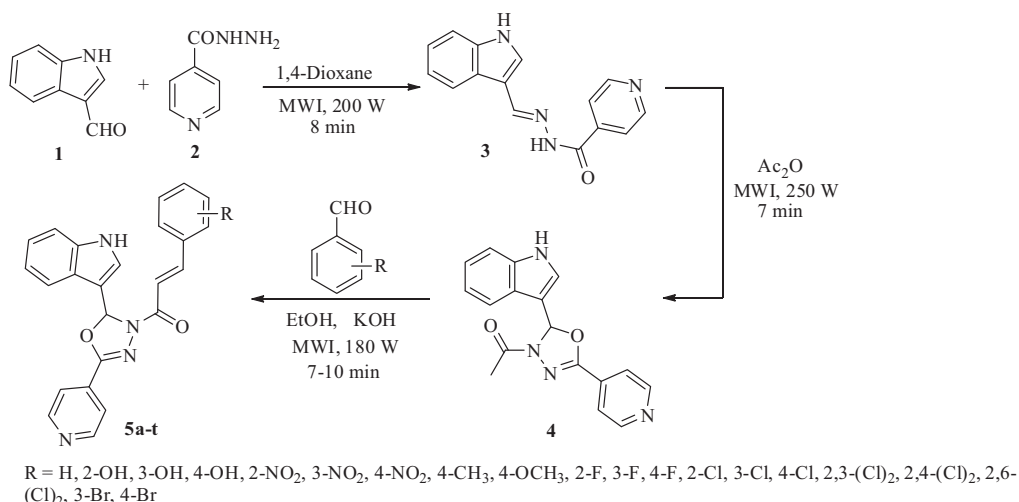
In an effort to prepare better therapeutic agents for the treatment of tuberculosis and in continuation to our previous work,<sup>30–34</sup> amalgamation of three biologically versatile heterocyclic scaffolds like indole, pyridine and 1,3,4-oxadiazole in single molecular platform was undertaken. To establish structure activity relationship and for the development of new antitubercular agents, the synthesized compounds were screened for their in vitro antitubercular activity against *Mycobacterium tuberculosis* H<sub>37</sub>Ra and *Mycobacterium bovis* BCG. Furthermore, molecular docking studies helped in revealing the mode of action of these compounds through their interactions with the active site of the *Mycobacterium tuberculosis* enoyl reductase (InhA) enzyme.

Synthesis of the target compounds **5a–t** was achieved through the pathway illustrated in Scheme 1. Indole-3-carbaldehyde (**1**) was taken as starting material and reacted with isoniazid (**2**) to afford *N*'-(1*H*-indol-3-yl)methyleneisonicotinohydrazide (**3**), which on cyclization with acetic anhydride yielded intermediate 1-(2-(1*H*-indol-3-yl)-5-(pyridin-4-yl)-1,3,4-oxadiazol-3(2*H*)-yl) ethanone (**4**). The intermediate obtained was heated with an appropriately substituted aldehyde derivatives in ethanol (99.9%) furnished the desired compounds **5a–t**. The structures of all these newly synthesized compounds **5a–t** were confirmed by IR, NMR, mass spectral and C, H, N elemental analyses and were in full agreement with proposed structures. Formation of final compounds **5a–t** were confirmed by characteristic IR spectrum absorption bands in the range of 3370–3420 cm<sup>−1</sup> and 1660–1680 cm<sup>−1</sup> corresponding to —NH stretching of indole and >C=O respectively. Singlets at  $\delta$  6.50–6.70 and 10.10–10.40 ppm in <sup>1</sup>H NMR correspond to protons of 1,3,4-oxadiazole and —NH of indole

respectively. The aromatic ring protons and  $\beta$ -unsaturated ketone were observed in the range of  $\delta$  6.90–8.10 ppm. Characteristic peaks at  $\delta$  167.0–167.5 ppm in <sup>13</sup>C NMR confirmed the presence of >C=O in  $\alpha,\beta$ -unsaturated ketone. The mass spectrum of **5a–t** revealed that observed molecular ion peaks were in agreement with molecular weight of respective compounds.

In a standard primary screen, all the newly synthesized compounds **5a–t** were evaluated for their in vitro antitubercular activity against *M. tuberculosis* H<sub>37</sub>Ra and *M. bovis* BCG at concentrations of 30, 10 and 3  $\mu$ g/mL using an established XTT Reduction Menadione assay (XRMA) and NR (Nitrate reductase) assay, respectively.<sup>34,35</sup> Compounds showing 90% inhibition of bacilli at or lower than 30  $\mu$ g/mL were selected for further dose response curve. The drugs in clinical use, rifampicin and isoniazid were used as reference. The results are reported in Table 1. In general, the newly synthesized compounds showed excellent selectivity towards *M. bovis* BCG compared to *M. tuberculosis* H<sub>37</sub>Ra. The antitubercular activity results suggested that none of the compounds showed any significant activity against *M. tuberculosis* H<sub>37</sub>Ra. Compounds **5b**, **5e**, **5g** and **5q** substituted with 2-OH, 2-NO<sub>2</sub>, 3-NO<sub>2</sub> and 2,4-(Cl)<sub>2</sub> functional groups displayed excellent MICs ranging from 0.94 to 5.17  $\mu$ g/mL against *M. bovis* BCG. Compound **5b** came out as the most active compound against active *M. bovis* BCG with MIC of 0.94  $\mu$ g/mL while, compound **5e** was most active against dormant *M. bovis* BCG with MIC of 0.85  $\mu$ g/mL. Compounds **5g** (active state MIC: 2.5  $\mu$ g/mL, dormant state MIC: 2.37  $\mu$ g/mL) and **5q** (active state MIC: 5.17  $\mu$ g/mL, dormant state MIC: 4.97  $\mu$ g/mL) were approximately 2–6-fold less active than the most active compounds **5b** and **5e**. From the standpoint of structure activity relationship, it was observed that the antitubercular activity was significantly affected by the substitution pattern at phenyl ring of chalcone moiety. It was observed that presence of —OH and —NO<sub>2</sub> functional groups at 2nd position of phenyl ring was favorable for enhanced antitubercular activity while any alteration in this substitution pattern witnessed a substantial decrease in antitubercular potency.

After identifying a good number of active antitubercular leads, cytotoxicity of all the newly synthesized compounds **5a–t** were tested against three human cancer cell lines, HeLa (human cervical cancer cell line), A549 (human lung adenocarcinoma cell line) and PANC-1 (human pancreas carcinoma cell line) using 3-(4,5-dimethylthiazol-2-yl)-2,5-diphenyltetrazoliumbromide (MTT) assay<sup>36–38</sup> with paclitaxel as a positive control. The cytotoxicity results presented in Table 2 are expressed in terms of GI<sub>50</sub> and



Scheme 1. Synthetic route for the preparation of title compounds **5a–t**.

**Table 1**  
Antitubercular screening results of compounds **5a–t**

Entry	R	Antitubercular activity against <i>M. tuberculosis</i> H <sub>37</sub> Ra ( $\mu\text{g/ml}$ )				Antitubercular activity against <i>M. bovis</i> BCG ( $\mu\text{g/ml}$ )			
		Active state		Dormant state		Active state		Dormant state	
		MIC <sup>c</sup>	IC <sub>50</sub> <sup>d</sup>	MIC	IC <sub>50</sub>	MIC	IC <sub>50</sub>	MIC	IC <sub>50</sub>
<b>5a</b>	H	>30	28.72	>30	>30	>30	12.33	>30	11.24
<b>5b</b>	2-OH	>30	>30	>30	>30	0.94	0.46	1.19	0.68
<b>5c</b>	3-OH	>30	>30	>30	>30	>30	>30	>30	>30
<b>5d</b>	4-OH	>30	>30	>30	>30	>30	28.81	>30	27.92
<b>5e</b>	2-NO <sub>2</sub>	>30	>30	>30	>30	1.03	0.48	0.85	0.36
<b>5f</b>	3-NO <sub>2</sub>	>30	>30	>30	>30	>30	>30	>30	>30
<b>5g</b>	4-NO <sub>2</sub>	>30	>30	>30	>30	2.50	1.42	2.37	1.37
<b>5h</b>	4-CH <sub>3</sub>	>30	>30	>30	>30	>30	>30	>30	>30
<b>5i</b>	4-OCH <sub>3</sub>	>30	>30	>30	>30	>30	>30	>30	>30
<b>5j</b>	2-F	>30	>30	>30	>30	>30	>30	>30	>30
<b>5k</b>	3-F	>30	>30	>30	>30	>30	19.54	>30	20.41
<b>5l</b>	4-F	>30	>30	>30	>30	>30	>30	>30	>30
<b>5m</b>	2-Cl	>30	11.62	>30	>30	>30	>30	>30	>30
<b>5n</b>	3-Cl	>30	2.54	>30	>30	>30	>30	>30	>30
<b>5o</b>	4-Cl	>30	>30	>30	>30	>30	>30	>30	>30
<b>5p</b>	2,3-(Cl) <sub>2</sub>	>30	>30	>30	>30	>30	>30	>30	>30
<b>5q</b>	2,4-(Cl) <sub>2</sub>	>30	29.34	>30	27.54	5.17	2.93	4.97	1.5
<b>5r</b>	2,6-(Cl) <sub>2</sub>	>30	12.68	>30	13.72	>30	>30	>30	19.23
<b>5s</b>	3-Br	>30	>30	>30	>30	>30	>30	>30	21.71
<b>5t</b>	4-Br	>30	>30	>30	>30	>30	>30	>30	>30
<b>RP<sup>a</sup></b>	—	0.041	0.0016	0.045	0.0017	0.015	0.0012	0.017	0.0015
<b>INH<sup>b</sup></b>	—	0.031	0.0013	0.034	0.0014	0.033	0.0012	0.037	0.0017

<sup>a</sup> RP: rifampicin.<sup>b</sup> INH: isoniazid.<sup>c</sup> MIC indicated minimum inhibitory concentration.<sup>d</sup> IC<sub>50</sub> indicates 50% inhibitory concentration.**Table 2**  
Cytotoxicity studies results of compounds **5a–t** in three human cancer cell lines<sup>b</sup>

Entry	Cytotoxicity against HeLa cell line ( $\mu\text{g/ml}$ )		Cytotoxicity against A549 cell line ( $\mu\text{g/ml}$ )		Cytotoxicity against PANC-1 cell line ( $\mu\text{g/ml}$ )	
	GI <sub>90</sub> <sup>a</sup>	GI <sub>50</sub> <sup>a</sup>	GI <sub>90</sub>	GI <sub>50</sub>	GI <sub>90</sub>	GI <sub>50</sub>
<b>5a</b>	>30	>30	>30	>30	>30	>30
<b>5b</b>	>30	26.81	>30	>30	>30	>30
<b>5c</b>	>30	>30	>30	>30	>30	>30
<b>5d</b>	>30	>30	>30	>30	>30	>30
<b>5e</b>	>30	>30	>30	>30	>30	>30
<b>5f</b>	>30	>30	>30	>30	>30	>30
<b>5g</b>	>30	>30	>30	>30	>30	>30
<b>5h</b>	>30	>30	>30	>30	>30	>30
<b>5i</b>	>30	>30	>30	>30	>30	>30
<b>5j</b>	>30	>30	>30	>30	>30	>30
<b>5k</b>	>30	>30	>30	>30	>30	>30
<b>5l</b>	>30	>30	>30	>30	>30	>30
<b>5m</b>	>30	>30	>30	>30	>30	>30
<b>5n</b>	>30	>30	>30	>30	>30	>30
<b>5o</b>	>30	>30	>30	>30	>30	>30
<b>5p</b>	>30	>30	>30	>30	>30	>30
<b>5q</b>	>30	29.34	>30	>30	>30	>30
<b>5r</b>	>30	>30	>30	>30	>30	>30
<b>5s</b>	>30	>30	>30	>30	>30	>30
<b>5t</b>	>30	>30	>30	>30	>30	>30
Paclitaxel	0.075 $\pm$ 0.03	0.005 $\pm$ 0.002	5.88 $\pm$ 0.3	0.12 $\pm$ 0.04	0.078 $\pm$ 0.02	0.0038 $\pm$ 0.002

<sup>a</sup> GI<sub>90</sub> and GI<sub>50</sub> indicates the 90% and 50% growth inhibition concentration, respectively.<sup>b</sup> Three cancer cell line—HeLa: human cervical cancer cell line, A549: human lung adenocarcinoma cell line and PANC-1: human pancreas carcinoma cell line.

GI<sub>50</sub> indicating the 90% and 50% growth inhibition concentration, respectively. None of the tested compounds exhibited any significant cytotoxic effects against HeLa, A549 and PANC-1 cell lines, suggesting a great potential for their in vivo use as antimicrobial agents.

The cytotoxicity assay returned a GI<sub>50</sub> value, which allowed selectivity indexes to be calculated.<sup>39–41</sup> The selectivity indexes reported in Table 3 were calculated by dividing GI<sub>50</sub> for cell lines

(HeLa, A549 and PANC-1) by the MIC against active/dormant *M. bovis* BCG. Compounds **5b**, **5e** and **5g** showed selectivity index of greater than 10 against all the three cell lines. Compounds with SI value  $\geq 10$  are considered safe for further screening, which makes compounds **5b**, **5e** and **5g** very promising antitubercular compounds.

Compounds **5a–t** were further screened for their antibacterial activity against four bacteria strains (Gram-negative strains:

**Table 3**Selectivity index (SI) of most active compounds **5b**, **5e**, **5g** and **5q** on human cell lines against active as well as dormant *M. bovis* BCG

Entry	<i>M. bovis</i> BCG MIC ( $\mu\text{g/ml}$ )		SI <sup>c</sup> against HeLa cell line		SI against 549 cell line		SI against PANC-1 cell line		Glide score	Glide energy
	Active state	Dormant state	Active state	Dormant state	Active state	Dormant state	Active state	Dormant state		
<b>5b</b>	0.94	1.19	28.52	22.53	>31.91	>25.21	>31.91	>25.21	−8.218	−53.122
<b>5e</b>	1.03	0.85	>29.12	>35.29	>29.12	>35.29	>29.12	>35.29	−8.267	−54.856
<b>5g</b>	2.5	2.37	>12	>12.65	>12	>12.65	>12	>12.65	−8.07	−48.658
<b>5q</b>	5.17	4.97	5.68	5.9	>5.80	>6.03	>5.80	>6.03	−7.639	−45.176
RP <sup>a</sup>	0.035	0.037	>2857.14	>2702.7	>2857.1	>2702.7	>2857.1	>2702.7	—	—
INH <sup>b</sup>	0.033	0.039	>3030.3	>2564.1	>3030.3	>2564.1	>3030.3	>2564.1	—	—

<sup>a</sup> RP: rifampicin.<sup>b</sup> INH: isoniazid.<sup>c</sup> Selectivity index (SI) was calculated for all the active compounds taking into account the MIC against active as well as dormant *M. bovis* BCG and the GI<sub>50</sub> on human cancer cell lines (SI = GI<sub>50</sub>/MIC) by the MTT assay. If the SI is  $\geq 10$ , then the compound is investigated further.

*Escherichia coli*, *Pseudomonas fluorescens*; Gram-positive strains: *Staphylococcus aureus* and *Bacillus subtilis*) to investigate their specificity against MTB.<sup>42</sup> The antimicrobial activity results are summarized in Table 4. Four most active anti-tubercular compounds (**5b**, **5e**, **5g** and **5q**) were further confirmed from their dose dependent effect against four bacteria strains. The most promising compound **5q** showed strong specificity against MTB as compared to **5b**, **5e** and **5g**. All the compounds except **5d**, **5k**, **5o** and **5q** showed good antibacterial activity against *Escherichia coli*, *Pseudomonas fluorescens*; *Staphylococcus aureus* and *Bacillus subtilis*, with MIC value varying from **7.86** to **201.51**  $\mu\text{g/ml}$ . Our results clearly indicate that target of **5q** is mycobacteria specific and that can be explored further for potential antitubercular drug.

Experimental observations were followed up with molecular docking studies, in which the most active compounds **5e**, **5b**, **5g** and **5q** were docked into the active site of mycobacterial enoyl reductase (InhA). The docking studies were performed with Glide (Grid-Based Ligand Docking With Energetics) program<sup>43,44</sup> incorporated in the Schrödinger molecular modeling package (Schrödinger, LLC, New York, NY, 2015). The promising experimental results for the antitubercular activity could not lead to the conclusion of

the exact binding mode of 1,3,4-oxadiazole derivatives into the mycobacterial target and the types of main binding forces governing the variation in observed binding affinity. With this purpose, we selected computer simulation experiments with molecular docking method to explore the interaction mechanism of most active 1,3,4-oxadiazole derivatives with mycobacterial enoyl reductase (InhA) enzyme. The 1,3,4-oxadiazole derivatives are reported to inhibit mycobacterial enoyl reductase (InhA).<sup>45–47</sup> The enoyl-ACP (CoA) reductase (FabI/ENR/InhA) is an important enzyme in the mycobacterial type II fatty acid biosynthesis pathway. This enzymatic inhibition is shown in the fast-growing model organism *Mycobacterium smegmatis* to inhibit mycolic acid synthesis and induce cell lysis.<sup>48</sup>

In the absence of available resources to carry out the enzymatic studies, in silico computational chemistry approaches like molecular docking have become essential to identify the targets for different ligands. The theoretical predictions from the molecular docking study were found to be in agreement with the experimentally observed antitubercular activity. All the four derivatives **5e**, **5b**, **5g** and **5q** were successfully docked into the active site of mycobacterial enoyl reductase (InhA). While relatively consistent

**Table 4**Antibacterial screening results of compounds **5a–t**

Entry	R	Antibacterial activity against Gram –ve bacteria in $\mu\text{g/ml}$				Antitubercular activity against Gram +ve bacteria in $\mu\text{g/ml}$			
		<i>E. coli</i>		<i>P. fluorescens</i>		<i>S. aureus</i>		<i>B. subtilis</i>	
		MIC <sup>c</sup>	IC <sub>50</sub> <sup>d</sup>	MIC <sup>c</sup>	IC <sub>50</sub> <sup>d</sup>	MIC <sup>c</sup>	IC <sub>50</sub> <sup>d</sup>	MIC <sup>c</sup>	IC <sub>50</sub> <sup>d</sup>
<b>5a</b>	H	50.51	10.26	51.31	11.06	42.24	11.86	45.44	12.66
<b>5b</b>	2-OH	>256	21.72	192.31	22.52	>256	23.32	>256	22.12
<b>5c</b>	3-OH	49.17	16.65	82.76	17.45	84.36	18.25	121.14	19.85
<b>5d</b>	4-OH	>256	>256	>256	45.05	>256	>256	>256	>256
<b>5e</b>	2-NO <sub>2</sub>	>256	18.39	>256	19.19	>256	21.05	>256	24.25
<b>5f</b>	3-NO <sub>2</sub>	173.65	19.19	55.71	20.87	93.15	21.67	85.96	22.39
<b>5g</b>	4-NO <sub>2</sub>	28.25	9.46	29.05	11.86	30.65	12.66	31.45	13.46
<b>5h</b>	4-CH <sub>3</sub>	7.86	3.33	8.66	4.13	9.46	5.73	10.26	6.53
<b>5i</b>	4-OCH <sub>3</sub>	182.18	13.99	101.42	15.69	88.09	7.72	156.46	15.72
<b>5j</b>	2-F	>256	25.58	>256	26.38	201.51	28.78	>256	31.98
<b>5k</b>	3-F	>256	>256	>256	>256	>256	>256	>256	>256
<b>5l</b>	4-F	>256	13.61	>256	7.33	>256	12.92	>256	15.59
<b>5m</b>	2-Cl	27.58	1.73	25.18	2.53	29.18	3.33	21.99	4.13
<b>5n</b>	3-Cl	>256	13.99	>256	12.12	>256	14.52	>256	19.32
<b>5o</b>	4-Cl	>256	>256	>256	>256	>256	>256	>256	>256
<b>5p</b>	2,3-(Cl) <sub>2</sub>	159.12	5.99	197.77	6.79	161.52	7.59	167.92	8.39
<b>5q</b>	2,4-(Cl) <sub>2</sub>	>256	>256	>256	>256	>256	>256	>256	>256
<b>5r</b>	2,6-(Cl) <sub>2</sub>	>256	14.79	>256	15.59	148.33	86.78	>256	19.19
<b>5s</b>	3-Br	18.25	2.39	19.05	3.19	21.05	2.01	22.65	4.74
<b>5t</b>	4-Br	>256	12.12	>256	10.39	>256	12.79	>256	15.19
AMP <sup>a</sup>	—	1.46	0.086	4.36	1.87	1.0	0.42	10.32	3.15
KAN <sup>b</sup>	—	1.62	0.13	0.49	0.014	>33.0	>30	1.35	0.37

<sup>a</sup> AMP: ampicillin.<sup>b</sup> KAN: kanamycin.<sup>c</sup> MIC indicated minimum inhibitory concentration.<sup>d</sup> IC<sub>50</sub> indicates 50% inhibitory concentration.

interactions were observed for all the molecules in regards to the central 1,3,4-oxadiazole ring, it was the interaction of the indole, pyridine and the variously substituted aromatic ring with the surrounding amino acid residues that caused the variation in the observed binding affinity for these derivatives. The lowest energy docking pose of **5e** revealed the presence of two crucial hydrogen bonding interactions with Pro156 (2.090 Å) and Lys165 (2.457 Å) through pyridine and indole rings respectively (Fig. 1). Such a hydrogen bonding interaction serves as 'anchor', guiding the 3D orientation of the ligand in the active site facilitating the steric and electrostatic interactions. Furthermore, the enhanced binding affinity of **5e** can also be attributed to the extensive chain of steric and electrostatic interactions with residues forming the active site of mycobacterial enoyl reductase (InhA). The compound **5e** was observed to be stabilized within the active site through strong van der Waals interactions observed with Leu218 (−1.520 kcal/mol), Ile215 (−2.779 kcal/mol), Met199 (−3.662 kcal/mol), Ile194 (−2.423 kcal/mol), Pro193 (−2.505 kcal/mol), Lys165 (−1.458 kcal/mol), Met161 (−3.178 kcal/mol), Tyr158 (−7.107 kcal/mol), Ala157 (−1.507 kcal/mol), Met155 (−1.503 kcal/mol), Phe149 (−5.763 kcal/mol), Asp148 (−1.782 kcal/mol), Met147 (−3.232 kcal/mol), Met103 (−2.973 kcal/mol), Phe97 (−2.139 kcal/mol), Gly96 (−1.055 kcal/mol) and Ile21 (−2.228 kcal/mol) residues while a series of favorable electrostatic interactions were observed with Asp261 (−1.92 kcal/mol), Asp234 (−1.880 kcal/mol), Glu220 (−1.322 kcal/mol), Glu219 (−1.503 kcal/mol), Glu210 (−1.569 kcal/mol), Glu209 (−1.493 kcal/mol), Gly208 (−1.042 kcal/mol), Met199 (−1.112 kcal/mol), Ile194 (−1.103 kcal/mol), Glu169 (−1.061 kcal/mol), Asn159 (−1.521 kcal/mol), Pro156 (−2.051 kcal/mol), Met155 (−1.857 kcal/mol), Asp150 (−1.179 kcal/mol), Asp148 (−1.633 kcal/mol) and Asp115 (−1.225 kcal/mol).

Docking of **5b** into the active site of mycobacterial enoyl reductase (InhA) revealed the presence of a similar chain of interactions as observed for **5e** (Fig. 2). Even **5b** was involved in a strong hydrogen bonding interaction with Pro156 at a distance of 2.152 Å through pyridine ring as observed for **5e**. However, it could form two additional hydrogen bonding interactions with Gly96 (2.467 Å) and Ile197 (2.339 Å) residues through 2-OH functionality on the aromatic ring and the indole ring respectively which could safely stabilize the ligand into the active site.

The compound **5b** showed significant van der Waals interactions with Leu218 (−1.345 kcal/mol), Ile215 (−2.647 kcal/mol), Ile202 (−1.590 kcal/mol), Met199 (−3.549 kcal/mol), Ile194 (−2.857 kcal/mol), Pro193 (−1.327 kcal/mol), Gly192 (−1.199 kcal/mol), Ala191 (−1.123 kcal/mol), Glu169 (−1.633 kcal/mol), Met161 (−1.556 kcal/mol), Tyr158 (−6.858 kcal/mol), Ala157 (−1.297 kcal/mol), Met155 (−1.610 kcal/mol), Phe149 (−4.328 kcal/mol), Met103 (−2.776 kcal/mol), Met98 (−1.173 kcal/mol) and Phe97 (−2.015 kcal/mol) residues in the active site. Further it formed favorable electrostatic interactions with Asp261 (−1.233 kcal/mol), Asp234 (−1.107 kcal/mol), Glu220 (−1.907 kcal/mol), Glu219 (−1.928 kcal/mol), Glu210 (−1.460 kcal/mol), Glu209 (−1.291 kcal/mol), Gly208 (−1.183 kcal/mol), Thr196 (−1.163 kcal/mol), Ile194 (−1.486 kcal/mol), Asn159 (−1.403 kcal/mol), Pro156 (−1.671 kcal/mol), Met155 (−1.479 kcal/mol), Asp150 (−1.900 kcal/mol), Asp148 (−1.625 kcal/mol), Asp115 (−1.311 kcal/mol) and Gly96 (−1.337 kcal/mol) residues lining the active site.

Compound **5g** showed the same binding mode as that of **5e** and **5b**, with the only difference of a relatively lower binding energy and consequently lower docking score (see Fig. 3). The per residue interaction analysis showed that the compound is involved in a chain of favorable van der Waals interactions with Leu218 (−1.171 kcal/mol), Ile215 (−2.145 kcal/mol), Met199 (−2.791 kcal/mol), Thr196 (−2.006 kcal/mol), Ile194 (−1.152 kcal/mol), Pro193 (−1.311 kcal/mol), Gly192 (−1.197 kcal/mol), Ala191 (−1.082 kcal/mol), Tyr158 (−3.809 kcal/mol), Ala157 (−1.048 kcal/mol), Met155 (−1.458 kcal/mol), Phe149 (−2.144 kcal/mol), Met103 (−2.095 kcal/mol), Ile21 (−2.602 kcal/mol) and Ser20 (−1.504 kcal/mol) residues in the active site. Furthermore it formed several good electrostatic interactions with Asp261 (−1.347 kcal/mol), Asp234 (−1.058 kcal/mol), Glu220 (−1.102 kcal/mol), Glu219 (−1.323 kcal/mol), Ala211 (−1.105 kcal/mol), Glu210 (−1.108 kcal/mol), Glu209 (−1.174 kcal/mol), Gly208 (−1.038 kcal/mol), Ile202 (−1.044 kcal/mol), Ile194 (−1.782 kcal/mol), Glu169 (−1.826 kcal/mol), Asn159 (−1.281 kcal/mol), Pro156 (−1.475 kcal/mol), Met155 (−1.680 kcal/mol), Asp150 (−1.358 kcal/mol), Asp148 (−1.711 kcal/mol) and Asp115 (−1.683 kcal/mol). A strong hydrogen bonding interaction with a distance of 2.280 Å, 2.280 Å and 2.259 Å was observed with Ser94, Pro156 and Ile194 residues

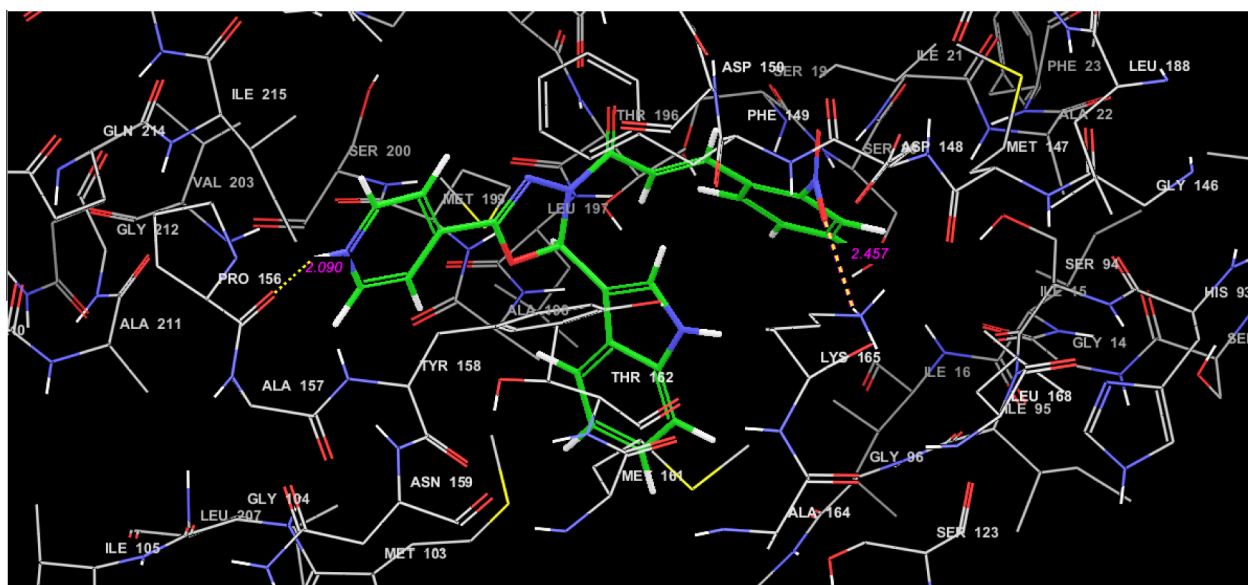
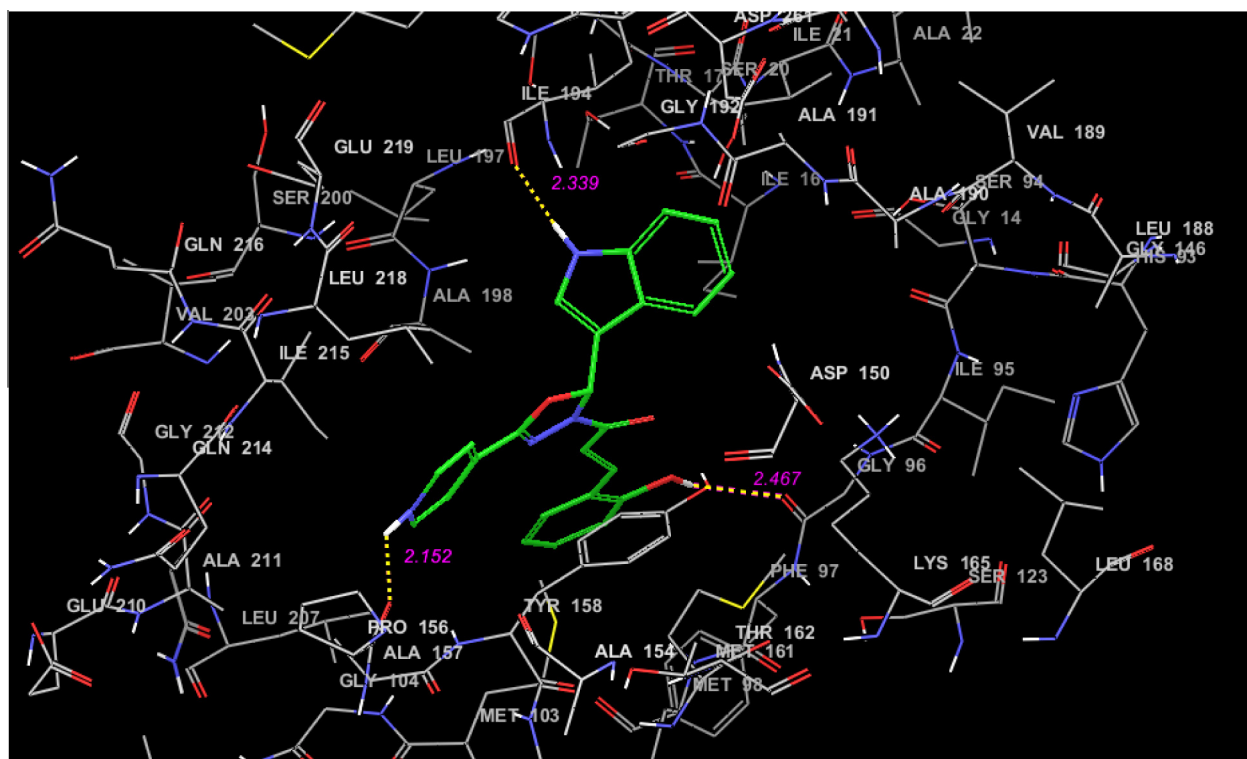
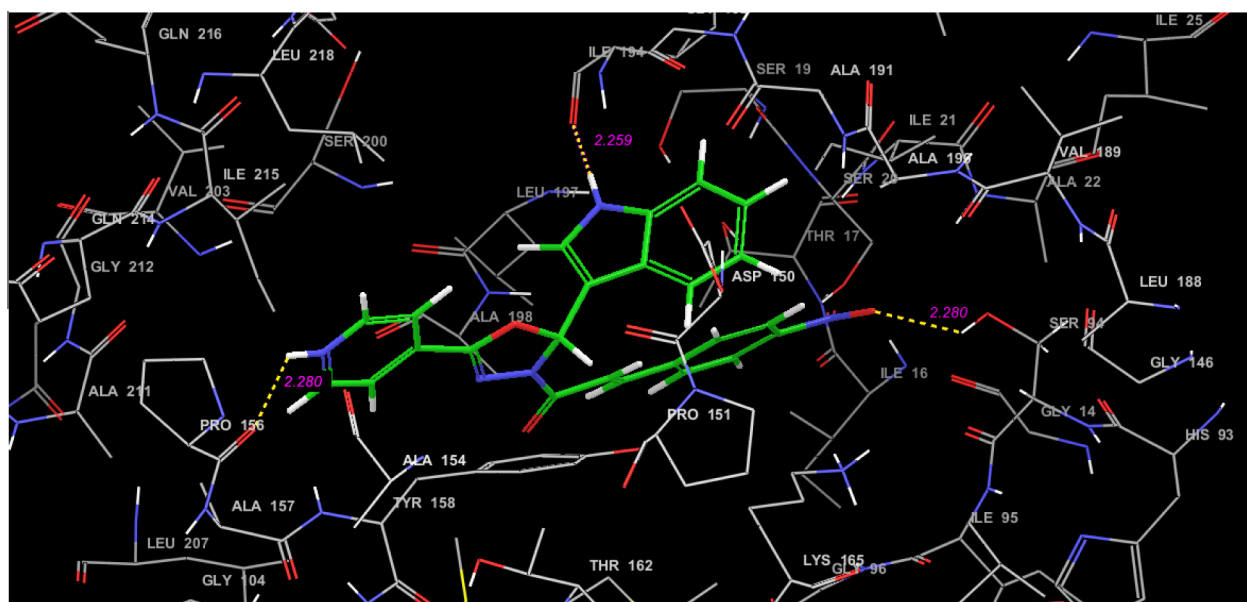


Figure 1. Binding mode of **5e** into the active site of MTB enoyl reductase (InhA).





**Figure 2.** Binding mode of **5b** into the active site of *MTB* enoyl reductase (InhA).



**Figure 3.** Binding mode of **5g** into the active site of *MTB* enoyl reductase (InhA).

respectively which could optimally place the compound in the active site.

Docking of **5q** revealed that it occupies the active site of InhA at the same coordinates as **5e**, **5b** and **5g** but with a relatively weaker affinity (see Fig. 4). The compound formed several van der Waals interactions with Leu218 (−1.047 kcal/mol), Ile215 (−2.118 kcal/mol), Leu207 (−1.095 kcal/mol), Ile202 (−1.150 kcal/mol), Met199 (−2.066 kcal/mol), Ile194 (−1.092 kcal/mol), Pro193 (−1.162 kcal/mol), Gly192 (−1.163 kcal/mol), Ala191 (−1.013 kcal/mol), Met161 (−1.162 kcal/mol), Tyr158 (−1.239 kcal/mol),

Met155 (−1.159 kcal/mol), Phe149 (−1.404 kcal/mol), Met103 (−1.970 kcal/mol), Met98 (−1.148 kcal/mol) and Phe97 (−1.090 kcal/mol) residues while favorable electrostatic interactions were observed with Asp261 (−1.121 kcal/mol), Asp234 (−1.339 kcal/mol), Glu220 (−1.267 kcal/mol), Glu219 (−1.527 kcal/mol), Ala211 (−1.018 kcal/mol), Glu210 (−1.727 kcal/mol), Glu209 (−1.409 kcal/mol), Gly208 (−1.194 kcal/mol), Thr196 (−1.192 kcal/mol), Ile194 (−1.707 kcal/mol), Glu169 (−1.034 kcal/mol), Asn159 (−1.492 kcal/mol), Pro156 (−1.829 kcal/mol), Met155 (−1.545 kcal/mol), Asp150 (−1.570 kcal/mol), Asp148

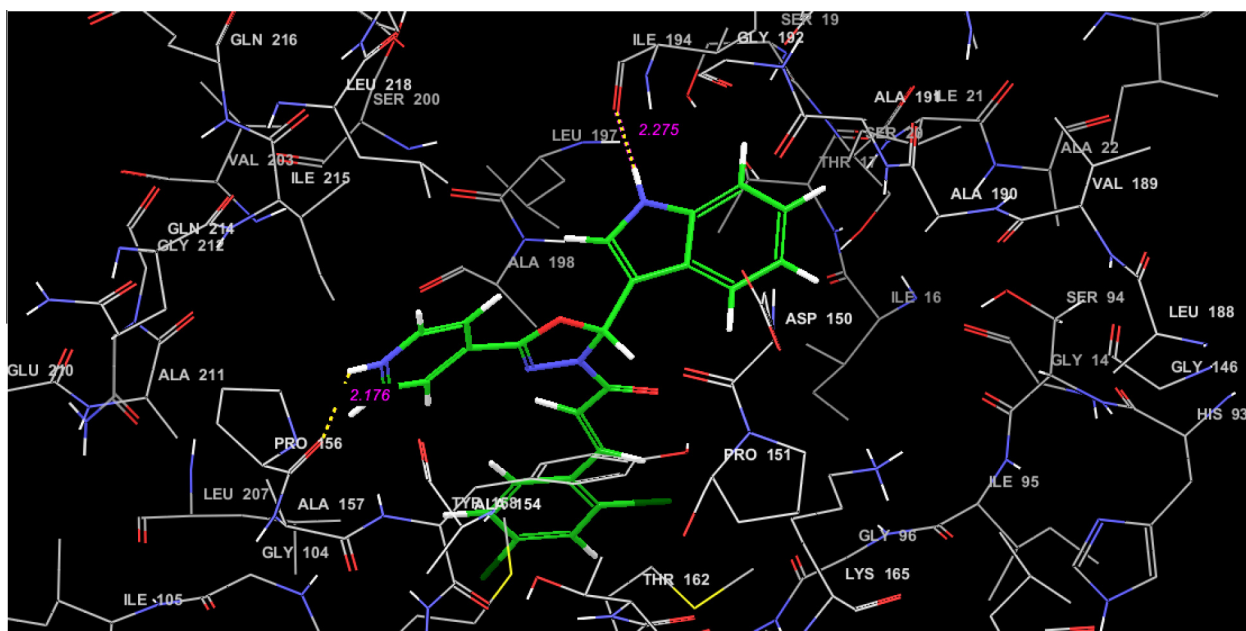


Figure 4. Binding mode of **5q** into the active site of MTB enoyl reductase (InhA).

(−1.192 kcal/mol) and Asp115 (−1.828 kcal/mol). A strong hydrogen bonding interaction with a distance of 2.176 Å and 2.275 Å was observed with Pro156 and Ile194 residues.

The per-residue interaction analysis revealed that the primary driving forces for mechanical interlocking between these 1,3,4-oxadiazole derivatives and the active site of the mycobacterial enoyl reductase (InhA) were the steric and electrostatic complementarities. Furthermore it could provide a quantitative insight into various non-bonded interactions (Steric and electrostatic) responsible for the variation observed in the binding affinity of these molecules which can guide site specific modification in these molecules to arrive at potent antitubercular candidates.

In summary, a series of novel indole and pyridine based 1,3,4-oxadiazole derivatives were efficiently synthesized and evaluated for their in vitro antimycobacterial potency against *M. tuberculosis* H<sub>37</sub>Ra and *M. bovis* BCG with higher selectivity towards the later. Among all the tested compounds, **5b**, **5e**, **5g** and **5q** were identified as the most active compounds from the study with MIC ranging from 0.94 to 5.17 µg/mL against *M. bovis* BCG. In the next step, all the newly synthesized compounds were evaluated for their cytotoxic effect against HeLa, A549 and PANC-1 cell lines and with the help of which, selectivity indexes for most active compounds **5b**, **5e**, **5g** and **5q** were calculated to determine their safety for further screening. Selectivity index values for compounds **5b**, **5e** and **5g** were ≥ 10 against all the cell lines which suggested that they are candidates for further screening. Specificity of compounds **5a–t** was checked by screening them for their antibacterial activity against four bacterial strains. Further, molecular docking investigation for the most active compounds **5b**, **5e**, **5g** and **5q** from the study was carried out into the active site of InhA which suggested that these compounds have a great potential for further optimization and development as antitubercular agents.

## Acknowledgements

The authors are thankful to the University Grants Commission, New Delhi for NON-SAP and UGC-BSR one-time grant and Department of Science and Technology, New Delhi for DST-FIST programs financial support. Authors A. R. Trivedi and Prakash C. Jha are

thankful to UGC, New Delhi for providing 'Dr. D. S. Kothari Post-Doctoral Fellowship' and start up grants respectively. Authors are also thankful to the Director of NCL Pune for providing biological screening of title compounds. We also thank Schrödinger Inc. for providing the Demo license of Schrödinger Suite and especially Vinod Devarji for delivering valuable technical support that has tremendously helped in this study.

## Supplementary data

Supplementary data associated with this article can be found, in the online version, at <http://dx.doi.org/10.1016/j.bmcl.2016.02.043>.

## References and notes

1. Espinal, M. A. *Tuberculosis* **2003**, 83, 44.
2. Nivin, B.; Nicholas, P.; Gayer, M.; Frieden, T. R.; Fujiwara, P. I. *Clin. Infect. Dis.* **1998**, 26, 303.
3. Goldman, R. C.; Plumley, K. V.; Laughon, B. E. *Infect. Disord. Drug Targets* **2007**, 7, 73.
4. Weltman, A. C.; Rose, D. N. *Arch. Intern. Med.* **1994**, 154, 2161.
5. Nguyen, L.; Thompson, C. J. *Trends Microbiol.* **2006**, 14, 304.
6. Pablos-Mendez, A.; Raviglione, M. C.; Laszlo, A.; Binkin, N.; Rieder, H. L.; Bustreo, F.; Cohn, D. L.; Lambregts-van Weezenbeek, C. S.; Kim, S. J.; Chaulet, P.; Nunn, P. N. *Engl. J. Med.* **1998**, 338, 1641.
7. Zumla, A.; George, A.; Sharma, V.; Herbert, R. H.; Baroness Masham of, I.; Oxley, A.; Oliver, M. *Lancet* **2015**, 3, e10.
8. Denhart, D. J.; Deskus, J. A.; Ditta, J. L.; Gao, Q.; Dalton King, H.; Kozlowski, E. S.; Meng, Z.; LaPaglia, M. A.; Mattson, G. K.; Molski, T. F.; Taber, M. T.; Lodge, N. J.; Mattson, R. J.; Macor, J. E. *Bioorg. Med. Chem. Lett.* **2009**, 19, 4031.
9. Shaveta; Singh, P. *Eur. J. Med. Chem.* **2014**, 74, 440.
10. Sharma, S. K.; Kumar, P.; Narasimhan, B.; Ramasamy, K.; Mani, V.; Mishra, R. K.; Majeed, A. B. *Eur. J. Med. Chem.* **2012**, 48, 16.
11. Mehndiratta, S.; Hsieh, Y. L.; Liu, Y. M.; Wang, A. W.; Lee, H. Y.; Liang, L. Y.; Kumar, S.; Teng, C. M.; Yang, C. R.; Liou, J. P. *Eur. J. Med. Chem.* **2014**, 85, 468.
12. Liew, L. P. P.; Fleming, J. M.; Longeon, A.; Mouray, E.; Florent, I.; Bourguet-Kondracki, M.-L.; Copp, B. R. *Tetrahedron* **2014**, 70, 4910.
13. Yamuna, E.; Kumar, R. A.; Zeller, M.; Rajendra Prasad, K. J. *Eur. J. Med. Chem.* **2012**, 47, 228.
14. Wang, X. M.; Xu, J.; Li, Y. P.; Li, H.; Jiang, C. S.; Yang, G. D.; Lu, S. M.; Zhang, S. Q. *Eur. J. Med. Chem.* **2013**, 67, 243.
15. Khidre, R. E.; Abu-Hashem, A. A.; El-Shazly, M. *Eur. J. Med. Chem.* **2011**, 46, 5057.
16. Prasanthi, G.; Prasad, K. V.; Bharathi, K. *Eur. J. Med. Chem.* **2014**, 73, 97.
17. Frolova, L. V.; Malik, I.; Uglinskii, P. Y.; Rogelj, S.; Kornienko, A.; Magedov, I. V. *Tetrahedron Lett.* **2011**, 52, 6643.

18. Brun, P.; Dean, A.; Di Marco, V.; Surajit, P.; Castagliuolo, I.; Carta, D.; Ferlin, M. *G. Eur. J. Med. Chem.* **2013**, 62, 486.
19. Jiao, Y.; Xin, B. T.; Zhang, Y.; Wu, J.; Lu, X.; Zheng, Y.; Tang, W.; Zhou, X. *Eur. J. Med. Chem.* **2015**, 90, 170.
20. Mahernia, S.; Adib, M.; Mahdavi, M.; Nosrati, M. *Tetrahedron Lett.* **2014**, 55, 3844.
21. Sun, J.; Zhu, H.; Yang, Z. M.; Zhu, H. L. *Eur. J. Med. Chem.* **2013**, 60, 23.
22. Desai, N. C.; Bhatt, N.; Somani, H.; Trivedi, A. *Eur. J. Med. Chem.* **2013**, 67, 54.
23. Harish, K. P.; Mohana, K. N.; Mallesha, L.; Prasanna Kumar, B. N. *Eur. J. Med. Chem.* **2013**, 65, 276.
24. Rajak, H.; Singh Thakur, B.; Singh, A.; Raghuvanshi, K.; Sah, A. K.; Veerasamy, R.; Sharma, P. C.; Singh Pawar, R.; Kharya, M. D. *Bioorg. Med. Chem. Lett.* **2013**, 23, 864.
25. Ahsan, M. J.; Samy, J. G.; Jain, C. B.; Dutt, K. R.; Khalilullah, H.; Nomani, M. S. *Bioorg. Med. Chem. Lett.* **2012**, 22, 969.
26. Guda, D. R.; Park, S. J.; Lee, M. W.; Kim, T. J.; Lee, M. E. *Eur. J. Med. Chem.* **2013**, 62, 84.
27. Guimaraes, C. R.; Boger, D. L.; Jorgensen, W. L. *J. Am. Chem. Soc.* **2005**, 127, 17377.
28. Abdel, R.; Farghaly, A. H. *J. Chin. Chem. Soc.* **2004**, 51, 147.
29. Swain, C. J.; Baker, R.; Kneen, C.; Moseley, J.; Saunders, J.; Seward, E. M.; Stevenson, G.; Beer, M.; Stanton, J.; Watling, K. *J. Med. Chem.* **1991**, 34, 140.
30. Khunt, R. C.; Khedkar, V. M.; Chawda, R. S.; Chauhan, N. A.; Parikh, A. R.; Coutinho, E. C. *Bioorg. Med. Chem. Lett.* **2012**, 22, 666.
31. Manvar, A.; Khedkar, V.; Patel, J.; Vora, V.; Dodia, N.; Patel, G.; Coutinho, E.; Shah, A. *Bioorg. Med. Chem. Lett.* **2013**, 23, 4896.
32. Samal, R. P.; Khedkar, V. M.; Pissurlenkar, R. R.; Bwalya, A. G.; Tasdemir, D.; Joshi, R. A.; Rajamohanan, P. R.; Puranik, V. G.; Coutinho, E. C. *Chem. Biol. Drug Des.* **2013**, 81, 715.
33. Radadiya, A.; Khedkar, V.; Bavishi, A.; Vala, H.; Thakrar, S.; Bhavsar, D.; Shah, A.; Coutinho, E. *Eur. J. Med. Chem.* **2014**, 74, 375.
34. Singh, U.; Akhtar, S.; Mishra, A.; Sarkar, D. *J. Microbiol. Methods* **2011**, 84, 202.
35. Khan, A.; Sarkar, D. *J. Microbiol. Methods* **2008**, 73, 62.
36. Mosmann, T. *J. Immunol. Methods* **1983**, 65, 55.
37. Ciapetti, G.; Cenni, E.; Pratelli, L.; Pizzoferrato, A. *Biomaterials* **1993**, 14, 359.
38. Sreekanth, D.; Syed, A.; Sarkar, S.; Sarkar, D.; Santhakumari, B.; Ahmad, A.; Khan, I. *J. Microbiol. Biotechnol.* **2009**, 19, 1342.
39. Protopopova, M.; Hanrahan, C.; Nikonenko, B.; Samala, R.; Chen, P.; Gearhart, J.; Einck, L.; Nacy, C. A. *J. Antimicrob. Chemother.* **2005**, 56, 968.
40. Poggi, M.; Barroso, R.; Costa-Filho, A. J.; de Barros, H. B.; Pavan, F.; Leite, C. Q.; Gambino, D.; Torre, M. H. *J. Mex. Chem. Soc.* **2013**, 57, 198.
41. Gundersen, L. L.; Nissen-Meyer, J.; Spilberg, B. *J. Med. Chem.* **2002**, 45, 1383.
42. Singh, R.; Nawale, L. U.; Arkile, M.; Shedbalkar, U. U.; Wadhwani, S. A.; Sarkar, D.; Chopade, B. A. *Int. J. Antimicrob. Agents* **2015**, 46, 183.
43. Friesner, R. A.; Banks, J. L.; Murphy, R. B.; Halgren, T. A.; Klicic, J. J.; Mainz, D. T.; Repasky, M. P.; Knoll, E. H.; Shelley, M.; Perry, J. K.; Shaw, D. E.; Francis, P.; Shenkin, P. S. *J. Med. Chem.* **2004**, 47, 1739.
44. Halgren, T. A.; Murphy, R. B.; Friesner, R. A.; Beard, H. S.; Frye, L. L.; Pollard, W. T.; Banks, J. L. *J. Med. Chem.* **2004**, 47, 1750.
45. Asgaonkar, K. D.; Mote, G. D.; Chitre, T. S. *Sci. Pharm.* **2014**, 82, 71.
46. Kini, S. G.; Bhat, A. R.; Bryant, B.; Williamson, J. S.; Dayan, F. E. *Eur. J. Med. Chem.* **2009**, 44, 492.
47. Mathew, B.; Suresh, J.; Mathew, G. E.; Sonia, G.; Krishnan, G. K. *Indian J. Pharm. Sci.* **2014**, 76, 401.
48. Vilcheze, C.; Morbidoni, H. R.; Weisbrod, T. R.; Iwamoto, H.; Kuo, M.; Sacchettini, J. C.; Jacobs, W. R., Jr. *J. Bacteriol.* **2000**, 182, 4059.